Draft version June 5, 2009
Preprint typeset using LaTeX style emulateapj v. 10/09/06

TIDAL STREAMS OF INTRACLUSTER LIGHT

Craig S. Rudick, J. Christopher Mihos, Lucille H. Frey[1]
Department of Astronomy, Case Western Reserve University, 10900 Euclid Ave, Cleveland, OH 44106

and

Cameron K. McBride
Department of Physics & Astronomy, Vanderbilt University, 6301 Stevenson Center, Nashville, TN 37235

(Received 2009 January 23; Accepted 2009 May 7)
Draft version June 5, 2009

ABSTRACT

Using N-body simulations, we have modeled the production and evolution of substructures in the intracluster light (ICL) of a simulated galaxy cluster. We use a density-based definition of ICL, where ICL consists of luminous particles which are at low densities, to identify ICL particles and track their evolution. We have implemented a friends-of-friends-type clustering algorithm which finds groups of particles correlated in both position and velocity space to identify substructures in the ICL, hereafter referred to as "streams". We find that $\approx 40\%$ of the cluster's ICL is generated in the form of these massive ($M \geq 7.0 \times 10^8$ M$_\odot$), dynamically cold streams. The fraction of the ICL generated in streams is greater early in the cluster's evolution, when galaxies are interacting in the group environment, than later in its evolution when the massive cluster potential has been assembled. The production of streams requires the strong tidal fields associated with close interactions between pairs of galaxies, and is usually associated with merging pairs of galaxies, or fast, close encounters with the cluster's central galaxy. Once streams are formed, they begin to decay as they are disrupted by the tidal field of the cluster. We find that streams have decay timescales which are ≈ 1.5 times their dynamical time in the cluster.

Subject headings: galaxies: clusters: general — galaxies: evolution — galaxies : interactions — galaxies: kinematics and dynamics — methods: N-body simulations

1. INTRODUCTION

Diffuse intracluster starlight (ICL) consists of stars in galaxy clusters which are observed to be outside of and distinct from the cluster galaxies. In the prevailing ΛCDM hierarchical mass assembly paradigm, the ICL is generated from the numerous gravitational interactions experienced by the cluster galaxies as they interact with other galaxies and the cluster potential during the cluster's formation and evolution. As a product of the dynamical interactions within the cluster, the ICL has the potential to reveal a great deal of information about the cluster's accretion history and evolutionary state. The quantity, morphology, and kinematics of the ICL each hold useful information related to the evolution of the cluster, as well as its constituent galaxies.

Observationally, ICL has been detected in numerous galaxy clusters through broadband imaging (e.g., Zwicky 1951; Uson et al. 1991; Vílchez-Gómez et al. 1994; Gonzalez et al. 2005; Mihos et al. 2005; Zibetti et al. 2005; Krick & Bernstein 2007) as well as the detection of discrete tracers, such as planetary nebulae (e.g., Feldmeier et al. 1998; Arnaboldi et al. 2004), red giants (e.g., Ferguson et al. 1998; Durrell et al. 2002; Williams et al. 2007a), and other types of stellar tracers (e.g., Neill et al. 2005; Gal-Yam et al. 2003; Williams et al. 2007b). Most studies estimate that the ICL comprises $\approx 10\% - 30\%$ of the clusters' luminosity. While it is now thought that ICL is a ubiquitous feature of evolved galaxy clusters, it is likely that there is no universal ICL fraction, but that different clusters will have different ICL contents, depending on its specific evolution and history (Murante et al. 2004; Conroy et al. 2007; Rudick et al. 2006, hereafter R06).

A number of observational studies have also shown that there is often distinct substructure found in the morphology of the ICL. These features can take numerous forms, including long straight streamers (Mihos et al. 2005), curved arcs (Trentham & Mobasher 1998; Calcáneo-Roldán et al. 2000), tidal tails (Krick et al. 2006), large plumes (Gregg & West 1998; Feldmeier et al. 2004), and bridges spanning galaxies (Feldmeier et al. 2002). However, due to the difficulty in quantifying the morphological characteristics of such substructures, descriptions of the their morphologies remain largely qualitative and imprecise.

While the existence of ICL is now well established, the processes which generate it are not well understood. There are a number of processes, however, which have been shown to be capable of stripping material from galaxies, including stripping during the initial collapse of the cluster (e.g., Merrit 1984); stripping of galaxies by an established cluster potential (Byrd & Valtonen 1990; Gnedin 2003); stripping within galaxy groups accreting onto the cluster (Mihos 2004, R06); and stripping from high speed encounters between cluster galaxies (Moore et al. 1996). In the complex environment of a collapsing and accreting galaxy cluster, all these processes likely contribute to the overall production of ICL.

Several recent studies have suggested that galaxy mergers are a primary mechanism responsible for generating ICL (Monaco et al. 2006; Stanghellini et al. 2006;

Electronic address: csr10@case.edu, mihos@case.edu, lfrey@lanl.gov
Electronic address: cameron.mcbride@vanderbilt.edu
[1] Now at Los Alamos National Laboratory, Los Alamos, NM, USA.

Conroy et al. 2007; Murante et al. 2007). Such merger processes leading to the creation of a diffuse stellar component are acting not only in massive galaxy clusters, but are also present in the hierarchical build-up of less massive structures, such as groups (Sommer-Larsen 2006) and even individual galaxy halos (Purcell et al. 2007). Several observational studies have seen evidence for diffuse, intergalactic light in galaxy groups (Nishiura et al. 2000; White et al. 2003; Da Rocha & Mendes de Oliveira 2005; Aguerri et al. 2006; Da Rocha et al. 2008), often involving significant substructure. On galactic scales, the substructure seen in the Milky Way's stellar halo (e.g., Harding et al. 2001; Johnston et al. 2008; Belokurov et al. 2006; Jurić et al. 2008) indicates that much of the Galaxy's stellar halo is the product of tidal disruption of satellite galaxies, analogous to the production of ICL in galaxy clusters.

In order to study to generation of ICL in clusters more directly, a number of recent studies have focused on simulating cluster evolution within a cosmological volume, where the ICL is traced by dark matter simulations tracer particles (e.g., Napolitano et al. 2003), collisionless galaxy models (R06), or full hydrodynamical models (e.g., Murante et al. 2004; Willman et al. 2004; Sommer-Larsen et al. 2005). These simulations have generally found that at $z = 0$, at least 10% of the clusters' stars were found in the diffuse ICL, in line with current observations. However, a direct comparison between the results of simulations and observations is complicated by the varying metrics used to define ICL in observations and simulations (see Section 3.1).

By combining both positional and kinematic data, we have the potential to dramatically increase our understanding of the ICL. Napolitano et al. (2003), Sommer-Larsen et al. (2005), and Willman et al. (2004) each study the kinematic distribution of the unbound stars and find significant kinematic substructure. Observationally, planetary nebulae studies have successfully measured line-of-sight velocities of intracluster stars in several galaxy clusters, including the Virgo (Arnaboldi et al. 2004) and Coma (Gerhard et al. 2005) clusters. Further studies, which include larger sample sizes, will allow the study of ICL substructure in phase space, many which may not detectable in position space alone.

In R06 we used a set of N-body simulations of galaxy clusters to measure the evolution of the ICL from an observational perspective. In this paper, we use one of these simulations to objectively identify and measure the evolution of substructure within the ICL. Section 2 gives an overview of the N-body simulation technique. In Section 3, we define a density-based definition of ICL, and describe the algorithm we have developed to identify ICL substructures; these substructures are referred to as "streams" throughout this paper. Section 4 measures the prevalence of streams within the ICL, while Sections 5 and 6 follow the evolution of individual galaxies and streams, respectively, in order to better understand the production and evolution of the streams. Finally, Section 7 contains a summary of our findings and a discussion of their implications.

2. THE SIMULATION

The simulation used to study the intracluster light in this paper was first described in R06; we reiterate only a brief outline of the simulation process here.

Our simulation technique begins by running a $N = 256^3$ $50 \times 50 \times 50$ Mpc $\Lambda = 0.7$, $\Omega_M = 0.3$, $H_0 = 70$ km s^{-1} Mpc^{-1} cosmological dark matter simulation from $z = 50$ to $z = 0$. From this simulation, we identify massive dark matter halos, with masses '10^{14} M$_\odot$, to resimulate at higher resolution. For each cluster, we identify the $z = 2$ halos which will later constitute the $z = 0$ cluster halo. Into these $z = 2$ halos we insert higher resolution collisionless galaxy models, substituting the most bound 70% of the original halo mass and leaving the remaining 30% to form an extended dark matter halo around the galaxy. For high-mass halos, we employ a "halo occupancy distribution" (HOD) technique (Berlind & Weinberg 2002), which allows us to populate single halos with multiple galaxy models; we also have a minimum halo mass, below which we do not insert a galaxy model. We use two types of galaxy models, initialized using the prescriptions of Hernquist (1993): a disk model in which the stars follow a composite exponential disk plus Hernquist (1990) bulge (with bulge-to-disk ratio of 1:5), and an elliptical galaxy model where the stars have a pure Hernquist (1990) distribution. The luminous particles which make up these galaxy models, and on which our analyses focus, have a mass of 1.4×10^6 M$_\odot$, with a gravitational softening length of 280 pc. Both models are embedded in isothermal dark halos consisting of particles of intermediate mass resolution, lower than luminous matter particles but higher than the original dark matter particles which make up the extended halo. The composite dark matter profile resulting from the particles in both the isothermal halo and the original extended dark matter distribution yields a flat rotation curve in the luminous disk, and exhibits a r^{-3} Navarro-Frenk-White (NFW)-like decline in density at large radius. Our galaxy models are scaled to match the mass of the substituted halo, and our galaxies have a total dark-to-luminous mass ratio of 10:1. Our final galaxy mass function behaves like a Schecter function with a high mass cutoff and at low masses shows a power law slope, $\alpha \approx -1$. With the $z = 2$ initialization complete, the cluster is evolved to $z = 0$ using the N-body code GADGET (Springel et al. 2001).

This technique allows us to study the detailed structure and evolution of the ICL in massive galaxy clusters in a cosmological environment, while keeping the simulations computationally feasible. We recognize, however, a number of caveats which need to be addressed when interpreting these results. Our collisionless galaxy models focus entirely on gravitational dynamics, while neglecting the various effects of hydrodynamics. We are thus isolating gravitational stripping as the mechanism driving ICL production, irrespective of the effects of star formation, ram pressure stripping, or other hydrodynamic processes. Also, in our galaxy substitution scheme, we have a minimum galaxy mass corresponding to 6×10^{10} M$_\odot$. For a Shechter luminosity function with faint end slope $\alpha = -1$, galaxies below this minimum mass contain about 10% of the cluster's total luminosity; we are unable to measure these galaxies' contribution to the ICL. Finally, we initialize our galaxy models into the dark matter halos which exist at $z = 2$. Although we use a mix of both elliptical and disk galaxy models, each initialized galaxy is in an identical evolutionary state (although

scaled in mass) as each other galaxy of the same type, ignoring the heterogeneity caused by the complexities of early galactic evolution. While most ICL formation is expected to take place at $z \leq 1$ (e.g., R06; Murante et al. 2007), any ICL formed at $z \geq 2$ (e.g., Saro et al. 2009) will be missed by our simulation technique. Our initialization at $z = 2$ also means that we only place galaxies into halos which meet our minimum halo mass criterion at that time, and not halos which only subsequently grow to reach that mass.

In this paper, we focus on a detailed analysis of one of one such cluster (cluster C2 from R06). At $z = 0$, the cluster has $R_{200} = 917$ kpc (the radius within which the density of the cluster is 200 times the critical density) and $M_{200} = 8.4 \times 10^{13}$ $M_\odot$ (the mass enclosed within R_{200}). The cluster is initialized with 144 galaxies, while only 95 remain at $z = 0$ due to galaxy mergers (see Section 3.2 for a more detailed discussion of mergers). 50 galaxies are inside of R_{200} at $z = 0$, containing 75% of the stellar mass in the simulation.

Figure 1 shows the evolution of this cluster, showing the smoothed surface mass density distribution of the cluster's luminous matter at four timepoints, roughly equally spaced in evolutionary time. The images were made in the same manner as those shown in R06, however here we have not converted the surface mass density into a surface brightness. The hierarchical assembly of the cluster can be clearly seen, and is of extraordinary importance in understanding all aspects of this cluster's evolution, including its ICL and ICL streams. Early in the cluster's history, at $t = 0.43$[2], there is not yet a central cluster, just a number of galaxy groups. The galaxies within these groups are merging and interacting with one another, but the groups themselves are still relatively independent of one another. What low surface density material (equivalent to the low surface brightness ICL from R06) there is, is concentrated around the small groups, and displays a number of long, linear features. As the cluster evolves, the galaxy groups begin to merge together to form the cluster. By $t = 0.62$, a number of groups have begun to merge and interact with one another, and by $t = 0.81$, a cluster core is clearly visible. The low surface density material has grown in extent around the cluster core, many of the linear structures seen at earlier evolutionary times have been destroyed by the cluster potential. These trends are continued until $t = 1$, where we see that the cluster has a central core with a large cD galaxy at its center, with a large extended envelope of low surface mass density material surrounding the core. On the far edges of the $t = 1$ image, several examples of galaxies which are well outside the cluster and have not yet had any significant interactions with the cluster potential can be seen. Understanding this hierarchical evolution will be extremely important when interpreting the evolution of the ICL and streams discussed in this paper.

3. DEFINING ICL AND STREAMS

3.1. *ICL Defined by Density*

There is no standard definition of ICL, and many authors have used different metrics to define and measure ICL in the literature. Common observational definitions of ICL include luminosity in excess of a fitted central galaxy profile (e.g., Gonzalez et al. 2005) or luminosity fainter than a given surface brightness limit (e.g., Feldmeier et al. 2004). In R06 we created simulated surface brightness maps of our clusters and measured the ICL content using the latter definition. However, any observationally tractable definition of ICL suffers from projection effects, and is therefore not well linked to the cluster physics. Most studies of ICL using numerical simulations have used a binding energy definition of ICL; i.e. ICL consists of stars which are not bound to any individual galaxy in the cluster potential (e.g., Napolitano et al. 2003; Murante et al. 2004; Sommer-Larsen et al. 2005). While this is an appealing definition from a theoretical perspective — since all stars are initially bound to their parent galaxy, unbound stars must have had physical forces act on them to change their binding energy — in practice, calculating the binding energy of particles requires making numerous assumptions about the mass distribution of the cluster and its galaxies. This can become especially difficult and convoluted during the complex merging processes which dominate the cluster's evolution at early times.

In this paper we have chosen to adopt a density-based definition of ICL which can be easily defined, repeatably measured, and intuitively understood throughout the cluster's evolution. The simplest form such a density-based definition of ICL would be to simply define a limiting density threshold, ρ_{thresh}, below which particles are considered ICL. We use a slightly modified version of this definition whereby we require ICL particles to remain below the density threshold for a minimum consecutive time period, t_{min}. This simple addendum helps to eliminate loosely bound particles on radial orbits around their host galaxy from being defined as ICL. Additionally, once we have identified a particle as ICL, it remains an ICL particle for the rest of the simulation, irrespective of its future density. This scheme for identifying ICL is premised on the simple model of ICL formation whereby particles are pulled from high to low density as they are stripped from their parent galaxies, and are thereafter unbound particles orbiting the cluster potential. We find that only a very small fraction of the particles we identify as ICL later become rebound to galaxies and are found in the high-density galactic cores, and do not affect the streams described in this paper.

Our ICL definition requires us to define a density threshold, ρ_{thresh}, below which particles are considered ICL. This choice is very similar to that faced in R06 where we defined ICL as luminosity below a given surface brightness threshold - namely, that the threshold choice is essentially arbitrary, but because we are defining ICL using a well-defined property, the measurement is extremely repeatable (see the end of Section 3.2 for more on the connections between density and surface brightness). As in R06, we have chosen a threshold value that attempts to select only what we have identified as ICL by eye and intuition. Figure 2 shows the density of particles from two example galaxies at z=0. Because we are primarily interested in tidal streams, we have chosen a threshold density of $\rho_{thresh} = 10^{-5}$ $M_\odot$ pc^{-3}, which we feel best separates the luminosity of the galaxy from that of the tidal streams clearly present in these galaxies.

[2] Unless otherwise specified, throughout this paper all times are given as a fraction of the age of the universe at $z = 0$.

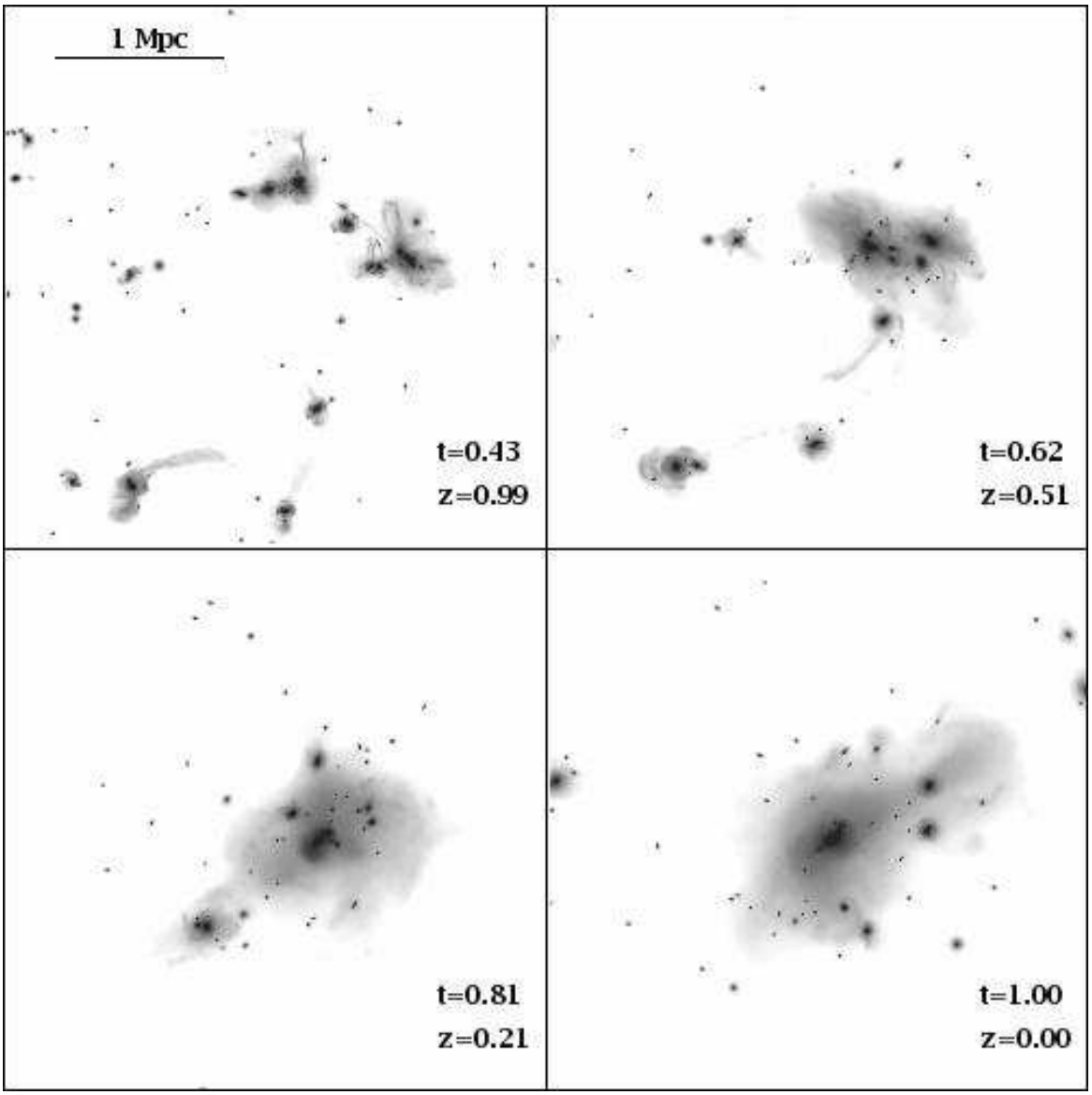

FIG. 1.— The cluster at four stages during its evolution. The gray-scale color is smoothed mass surface density of the cluster's luminous matter. There is no calibration of the gray-scale color, but is meant to show only relative surface density, and was chosen to highlight important features of the cluster. The physical scale of all four images is identical, and shown by the bar in the upper left of the figure. Each image is labeled by the time (in units of fraction of the age of the universe), t, and redshift, z, in the lower right.

While there is no single obvious value of ρ_{thresh} which is ideal for all galaxies in all environments, we find that higher values tend to classify too many particles in the outskirts of galaxies as ICL, whereas lower values miss particles which are clearly important contributors to the ICL. The density of each particle is defined as the mass density of luminous particles within the distance to that particle's 100-th nearest neighbor.

Our ICL definition also contains minimum time, t_{min}, to ensure that we do not label particles as ICL which are only in a short, transitory low-density state as they orbit in the outskirts of a galaxy. We have set $t_{min} = 200$ Myr, which is comparable to the dynamical timescale of the galaxies in our simulations. We feel that this criterion makes our definition more robust, and adding the minimum time criterion reduces the number of particles identified as ICL by only $\approx$ 10% – 15% and does not have a significant impact on our conclusions. In order to determine whether particles which become ICL near the end of the simulation satisfy the t_{min} criterion, we have evolved our simulation for a short time past $z = 0$ in order to measure the particle densities.

We find that a very small fraction of the luminous mass of our galaxies, $\approx 0.2\%$, is classified as ICL when we initialize the cluster at $z = 2$, before any evolution has taken place. This material is, for the most part, comprised of loosely bound particles on the outskirts of the most massive elliptical galaxies. However, Figure 3, which shows the distribution of particle densities at $z = 0$ and $z = 2$ for cluster C2, clearly shows that this is a minor correction and that this contribution is dwarfed by the ICL that is generated during the evolution of the cluster. Figure 3 also shows that our choice of $\rho_{thresh} = 10^{-5}$ corresponds to what appears to be a secondary peak in the $z = 0$ density distribution. While it is possible that this peak is the result of a discrete population of stellar particles at low density corresponding to the ICL, we have examined the particle distributions as a function of density

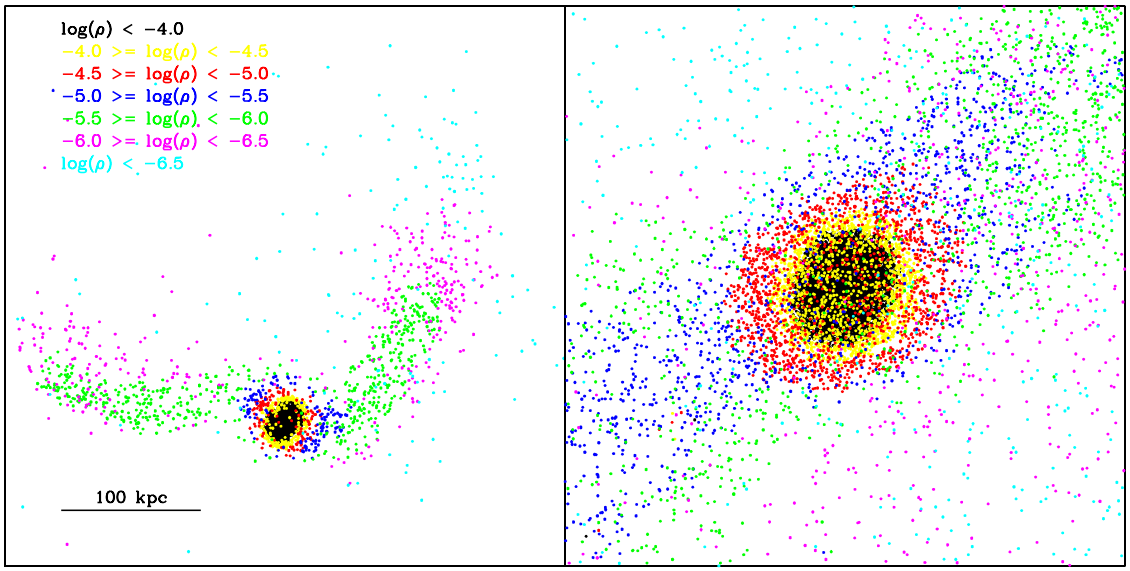

FIG. 2.— Two-dimensional projections of two galaxies at $z = 0$, showing the density of their luminous particles in various colors, as labeled by the key in the upper left. All densities are in units of $M_\odot$ pc^{-3}. The galaxy on the left is a low-mass disk galaxy, and the galaxy on the right is a high-mass elliptical merger product. Both galaxies are plotted on the same physical scale, as shown in the lower left. For clarity, only 10% of the particles are shown for the galaxy on the right.

and found no evidence that this is the case. The value of ρ_{thresh} was chosen based on an examination of tidal structures on galactic scales as described above, and is independent of the details of this secondary peak in the density distribution.

Thus, although any ICL definition includes trade-offs, we feel that our density-based definition is advantageous in that it is a simple, rigorous measurement, containing only well understood caveats. One downside to both a density and a binding energy definition of ICL is that neither is observationally tractable. The calculation of density requires full three-dimensional position information for all ICL stars, and binding energy requires full three-dimensional velocity information, plus a detailed knowledge of the dark matter mass distribution of galaxies. However, a density-based definition of ICL has the advantage of being analogous and closely related to the observationally tractable surface density or surface brightness definition of ICL.

3.2. *ICL Streams*

We have identified ICL streams as groups of ICL particles which are clustered in phase space. The clustering algorithm used to detect the streams is based on the DBSCAN algorithm (Ester et al. 1996) and is essentially a friends-of-friends (FOF) spatial clustering algorithm with an added free parameter which is used to reduce the inclusion of "noise" points from the clusters. Whereas a traditional FOF algorithm links together all points separated by less than a pre-defined linking length, ℓ, the DBSCAN algorithm first separates the data into "core" and "border" points based on the local density. Core points are high density points with k or more data points whose distance is less than ℓ; border points have fewer than k points with distance less than ℓ. The algorithm then proceeds in much the same way as a FOF algorithm, linking points separated by a distance less than ℓ, except that clusters are made up of only linked core points and the border points which are linked to these core points. Essentially, the DBSCAN algorithm is more restrictive than a FOF algorithm by eliminating the connections between border points. Generally, this can have the effect of reducing the size of clusters as compared with FOF, especially near the cluster's borders where the local density may be lower, or of splitting FOF clusters into multiple pieces by eliminating the border point connections between clusters. Note that by setting $k = 1$, the DBSCAN algorithm is identical to FOF. In both the FOF and DBSCAN algorithms, all points which are not linked to a cluster are considered "noise" points and do not belong to any cluster. The number of clusters is not pre-determined, and clusters can be of arbitrary shape, containing any number of data points greater than k.

In both the FOF and DBSCAN algorithms, the distance between points need not be the Euclidean distance, but can be any suitable metric, so long as the distance between each pair of points is well-determined. Because we are looking for tidal streams resulting from galaxy interactions as the galaxy cluster evolves, we expect that the luminous particles that we are seeking to cluster will be correlated in both position and velocity space. We have thus defined a phase space distance metric, Δw, that combines both position and velocity information to determine the phase space distance between a pair of points:

$$\Delta w = \sqrt{\left(\frac{|\Delta\vec{x}|}{x_n}\right)^2 + g\left(\frac{|\Delta\vec{v}|}{v_n}\right)^2} \qquad (1)$$

where $|\Delta\vec{x}|$ is the distance in position space and $|\Delta\vec{v}|$ is the distance in velocity space between the pair; x_n and v_n are normalization factors for the position and velocity, respectively; and g is used as a weighting factor to change the relative contributions of the position and velocity terms. We have set the values of the normalization factors to be $x_n = 10$ kpc and $v_n = 30$ km s^{-1}, since these are scales characteristic to kinds of tidal streams for which we are searching (e.g., Hibbard & Mihos 1995).

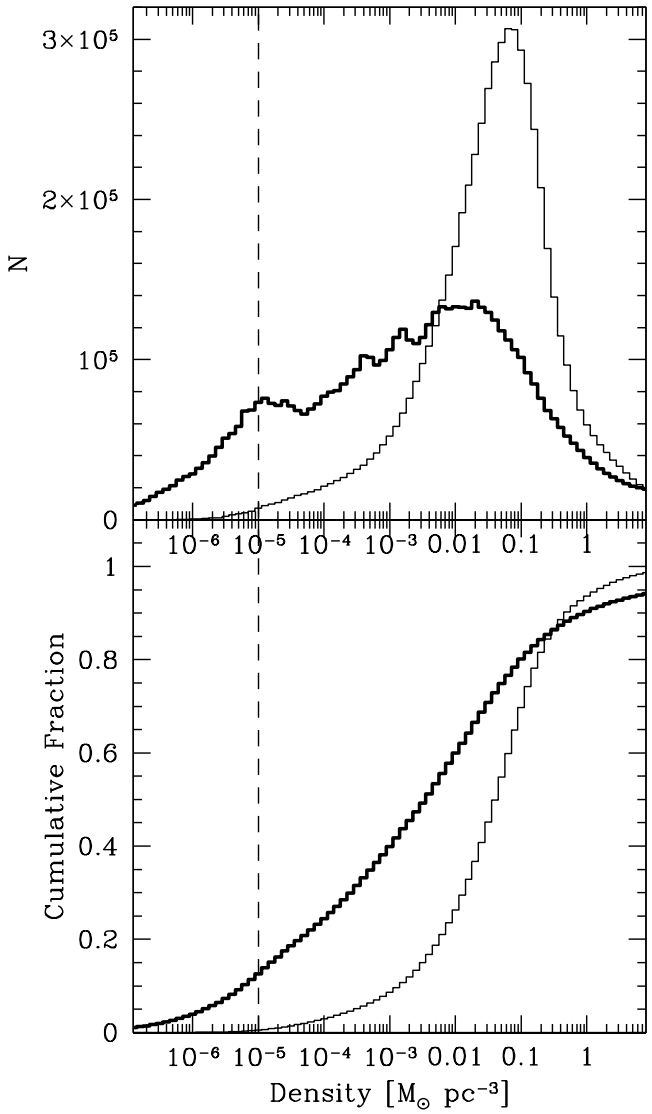

FIG. 3.— Top: the histogram of the number of luminous particles as a function of density at $z = 2$ (thin line) and $z = 0$ (thick line). Bottom: the cumulative histogram of the fraction of luminous particles at or above the given density at $z = 2$ (thin line) and $z = 0$ (thick line). The vertical dashed line indicates the value of ρ_{thresh}.

However, note that these normalizations merely provide a convenient starting point for choosing the values of g and ℓ, which, along with k, fully determine the clustering results.

Our testing revealed that most of the clustering is determined by the position information of the particles, i.e., the ICL particles are more clustered in position space ($g = 0$), than in velocity space ($g \to \infty$). However, including both the position and velocity in the clustering ($0 < g \ll \infty$) greatly improved the quality of the clustering results. We determined the "best" values for the free parameters, ℓ, k, and g, by comparing the clustered points to features in the simulations that we visually identified as tidal streams. For all the following analyses we used values of $\ell = 3.0$, $k = 20$, and $g = 1.0$. While our algorithm is able to detect clustered streams consisting of as few as 21 particles (the minimum cluster size is $k + 1$), we have limited the results to streams that contain a minimum of 500 particles, corresponding to a stellar mass of $7.0 \times 10^8 M_\odot$, in order to limit our results to only the largest, most robust streams.

Tidal streams which have been stripped from galaxies during the process of cluster evolution should consist primarily of particles from the same parent galaxy. It would be quite unlikely, given the high velocity dispersion of cluster galaxies, that two cold streams from different galaxies would merge to occupy the same phase space. Thus, in order to find these streams we have run our stream-finding algorithm independently on each galaxy in the cluster. The benefit of this approach is that the stream-finding algorithm is no longer influenced by the confusing effects of streams from other galaxies or the diffuse cluster ICL. That is, the environmental density in which the stream is located has no effect on its ability to be detected — this would be especially problematic at late times in the cluster's evolution when the interior of the cluster is densely populated by diffuse ICL. Thus, while our algorithm defines coherent streams of ICL clustered in phase space, it is unable to determine how distinct the streams are from the global ICL distribution.

When the simulation is initialized, each luminous particle is laid down as a member of a specific galaxy. However, in order to identify streams from a galaxy which is the product of merger of two or more initialized galaxies, we have developed a simple scheme to track the evolution of galaxies which have merged during the course of the simulation. We define a pair of galaxies to have merged when the separation between the pair becomes less than 5 kpc, and remains less than this distance for a minimum of 200 Myr. To calculate the galaxy separation, we define the position of each galaxy to be the density-weighted mean position of its luminous particles. When the pair merges, we identify the product as a new galaxy, consisting of all the non-ICL particles that were initialized with the precursor galaxies; the precursor galaxies themselves are no longer considered. For ICL particles, however, we identify a particle's parent galaxy as the galaxy to which the particle belonged at the moment it became ICL. Thus, it is often the case that we identify an ICL stream as having originated from a galaxy which has subsequently merged, and can therefore no longer generate ICL or streams. This scheme allows us to properly track the evolution of streams generated prior to a merger, while also allowing us to identify streams which originate from the merger product.

Figure 4 shows some examples of the streams which we have identified using this algorithm. The streams display a wide range of morphologies, from long thin tidal tails (e.g., the red stream from galaxy G2), to more diffuse plume-like structures (e.g., the red and blue streams in galaxy G3). These streams also span a wide range in masses from just above our minimum mass limit of 500 particles ($7.0 \times 10^8 M_\odot$, e.g., , G1 red, G2 green) to over an order of magnitude larger (e.g., G2 blue). Galaxies G1 and G4 display interesting examples of obvious tidal features which are present, but our algorithm does not classify them as streams. The tidal arm on the left of galaxy G1 is not massive enough to be a stream; our algorithm finds a group of only ≈ 450 particles, just under the minimum stream mass. The long tidal tail to the right of galaxy G4, however, is simply too low in

density for the particles to be grouped together by our algorithm. Section 5.1 contains a more thorough discussion of the histories of galaxies G1-G3 and the processes which create the streams seen here.

Because surface brightness is related to the surface mass density (or column density), we can calculate the surface brightness of material at a given density at various column depths, assuming a mass to light ratio. Following the assumptions of R06, where each particle has a V-band mass-to-light ratio of 5 in solar units, characteristic of an old stellar population, material at a density of ρ_{thresh} would have a surface brightness of 30.6 mag arcsec^{-2} through a 10 kpc column and 28.1 mag arcsec^{-2} though a 100 kpc column. While these surface brightnesses are somewhat lower than the $\mu_V = 26.5$ mag arcsec^{-2} ICL limit used in R06, in the cluster core we may observe material through even larger column depths, thus raising the surface brightness. Observationally, however, this suggests that small streams, with column depths of ≈ 10 kpc, may not be detectable through broadband imaging (e.g., Mihos et al. 2005). Such low surface brightnesses may only be accessible using discrete stellar tracers, such as planetary nebulae (e.g., Aguerri et al. 2005). These objects, however, have the advantage that they can be used to provide kinematic information (e.g., Arnaboldi et al. 2004), which can be useful in identifying ICL streams.

4. THE CONTRIBUTION OF STREAMS TO THE ICL

One important question about the formation ICL is the physical mechanism by which it is generated. If the ICL is created predominantly through the strong tidal forces caused by close interactions between pairs of galaxies or between small galaxy groups, then we would expect to see much ICL initially appear as large tidal streams. These types of interactions will generate ICL in short, discrete bursts, conducive to producing massive, dense tidal streams. If, however, the dominant mechanism is the slow, gradual stripping of material as a galaxy orbits in the cluster potential, then we would not expect to see such features contributing significantly to the ICL. The ICL resulting from such interactions would be more evenly distributed throughout the cluster, with few of the dense concentrations characteristic of tidal streams.

The top of Figure 5 shows the fraction of the cluster's luminous particles identified as ICL — the ICL fraction — and the fraction of the luminous particles identified as members of streams — the stream fraction — as a function of time. In order to focus only on the ICL and streams within the cluster itself, we have restricted this analysis only to particles which originate from galaxies which are found within the cluster's virial radius (R_{200}) at $z = 0$. The ICL fraction, by definition, is constrained to be monotonically increasing as a function of time. At $z = 0$ we find that 21% of the cluster's luminous particles are ICL. Outside the cluster virial radius, where galaxies are found predominantly in small groups with weak potentials, only 5% of the luminous particles are identified as ICL at $z = 0$.

The stream fraction of the cluster rises until $t \approx 0.6$, after which it begins to decrease somewhat. This roughly coincides with the time that the large pre-cluster groups begin to collapse to form a cluster core, as seen in Figure 1. The decrease in the stream fraction is a result of the fact that it is dependent on the rates of two competing processes — the production of new streams from tidal interactions and the destruction of old streams as they dissolve in the cluster potential, to form the diffuse ICL envelope. In order to disentangle these two competing effects, we have isolated the production of streams by calculating the fraction of the cluster's particles which have *ever* been a member of a stream, thereby ignoring the dissolution of streams. This analysis is premised on the simple model of stream formation whereby when a particle is stripped from a galaxy to become ICL, it does so either as part of a stream or as diffuse ICL, and after the initial stripping event, or dissolution of its stream, the particle will become part of the diffuse ICL and no longer contribute to any stream. We find these to be good assumptions for the vast majority of our particles.

To further investigate these trends, the middle of Figure 5 shows the time derivatives of the ICL fraction and the fraction of particles ever in a stream which are equivalent to the production rates of ICL and streams, respectively. Before $t \approx 0.6$, the streams production rate tracks the ICL production rate quite closely. Thus, early in the cluster's history, when the cluster core has yet to form and the galaxies are found predominantly in infalling groups, a large portion of the ICL produced is created in streams. However, later in the cluster's history the correlation between ICL and stream production grows much weaker. This indicates that much less of the ICL is being generated in streams as the cluster core is formed and the cluster potential deepens.

These trends are measured more directly in the bottom of Figure 5 where we show the ratio of the production rate of steams relative to ICL. Once again, the curve seems to display two distinct phases of evolution — before and after $t \approx 0.6$, when the cluster core begins to form. Although the ratio of production rates is quite noisy, it is apparent that early in the cluster's history, $\approx 60\%$ the ICL produced is generated in streams, whereas by the end of its' evolution, only $\approx 25\%$ of the cluster's ICL is generated in streams. Also shown in the bottom of Figure 5 are the ratios of the stream fraction to ICL fraction, and the fraction of particles which have ever been in a stream relative to the ICL fraction. Both curves peak in the $t \approx 0.5 - 0.6$ range, and by $z = 0$ we find that while $\approx 40\%$ of the cluster's ICL was originally generated in streams, only $\approx 5\%$ of the cluster's ICL is *currently* in a stream.

These data clearly show that early in the cluster's history, when most galaxies are still living in the pre-cluster group environment, most ICL is generated in the form of streams, whereas once the massive cluster potential has formed at later times, streams are created much less efficiently. The following sections will look more closely at the role of the environment in determining the galactic interactions that generate streams, and the environment's effect on the streams themselves.

5. THE GALACTIC ORIGINS OF ICL STREAMS

In order to understand the processes which create massive ICL streams, we have closely followed the evolution of individual galaxies within the cluster, in order to determine when and how they create these streams. As galaxies merge, orbit, and evolve in the cluster potential, they are continuously undergoing an extraordinary

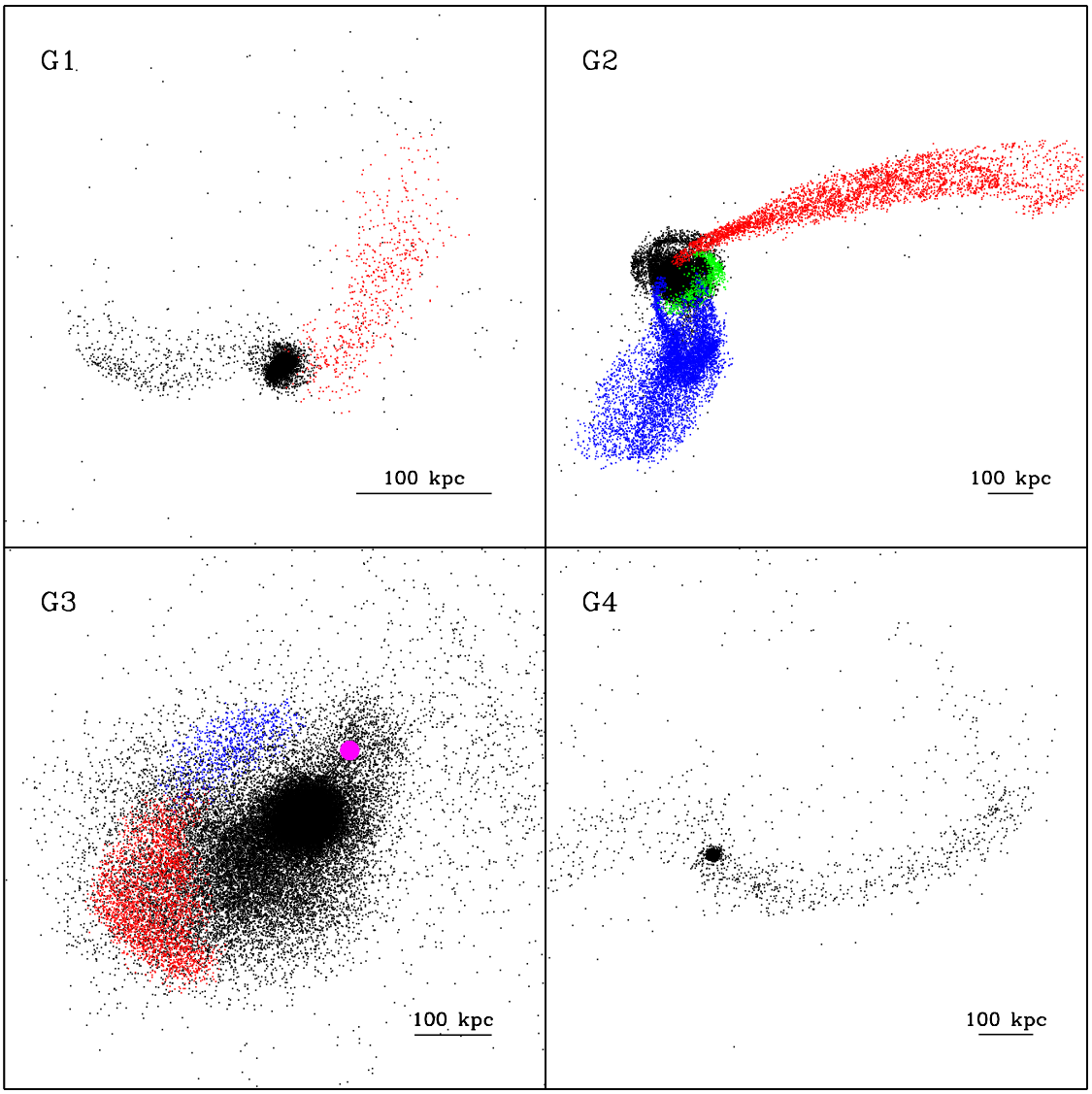

FIG. 4.— The subfigures each represent a two-dimensional projection of one galaxy from the simulation, labeled G1–G4, respectively. In black are non-stream luminous particles from the galaxies; for clarity, only 10% of these particles are plotted for galaxies G2 and G3. In red, blue, and green are individual streams identified by our algorithm from the galaxies. The bar in the lower right of each figure shows the physical scale. The magenta circle in galaxy G3 marks the location of the cD.

range of interactions that are difficult to quantify in an unambiguous way. Therefore, here we will concentrate on creating a qualitative description of the types of interactions which are affecting galaxies and the effects of these interactions on the production of streams. Again, "streams" here refers to massive, dense, dynamically cold structures found by the algorithm described in Section 3.2.

Figure 6 shows, for each galaxy, the fraction of the galaxy's ICL which was produced in streams (the stream production efficiency), versus the galaxy's cluster-centric radius at $z = 0$. In general, the galaxies can be divided into two categories, galaxies ending up within the cluster's virial radius (defined as R_{200}), and those outside. Outside the virial radius, galaxies that did not undergo a merging event (singleton galaxies) generated no streams whatsoever. Galaxies that did merge show a wide spread in stream production efficiency, from $\approx$ 0% to 60%. Within the virial radius of the cluster, the stream production efficiencies of merged galaxies are very similar to those of the more distant merged galaxies. However, a number of singleton galaxies within the cluster virial radius have produced streams, with efficiencies ranging from $\approx$ 0% to 80%.

The differences between these sets of galaxies are due to the different conditions which the galaxies experience during their evolution. The creation of massive streams requires strong tidal fields which are able to strip large amounts of mass from galaxies over short periods of time. For galaxies that undergo mergers, the most significant tidal interactions are likely to be those between the merging pairs of galaxies themselves. These forces are relatively independent of the local environment beyond the merging pair, and should thus be similar for galaxies both near and far from the cluster center. However, by the large spread in stream production efficiency seen within the set of merged galaxies, we see that the details of the merger process can vary considerably and have a pro-

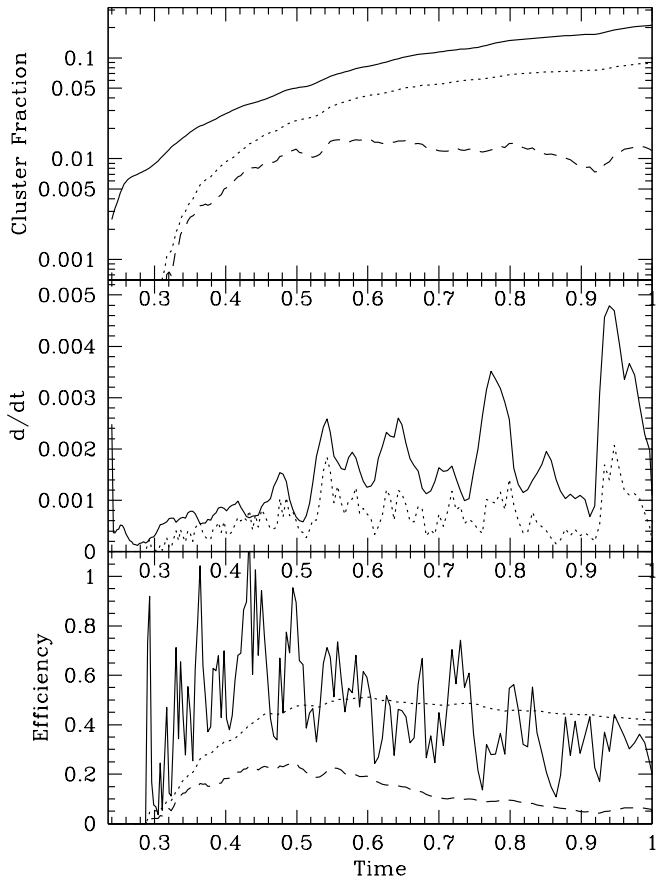

FIG. 5.— Top: the ICL fraction (solid), stream fraction (dashed), and fraction of particles which have ever been in a stream (dotted) as a function of time. Middle: the ICL production rate (solid) and streams production rate (dotted) as a function of time. Bottom: the fraction of the cluster's ICL which is in streams (dashed) or has ever been in a stream (dotted) as a function of time. Also shown is the ratio of the stream production rate to the ICL production rate (solid), as a function of time. The time axis is in units of fraction of the age of the universe (as in R06). See the text for more details.

found effect on the merger's ability to create streams. Unlike merged galaxies, singleton galaxies must have another massive potential — such as the cD galaxy at the core of the galaxy cluster — to interact with in order to create streams. Galaxies that end up within the cluster's virial radius are much more likely to have had such an interaction with a massive galaxy; thus singleton galaxies outside the cluster virial radius have not produced any streams. Not all galaxies within the cluster virial radius have produced streams, however. This is due to a number of effects. First, the strength of the tidal field is dependent on the gradient of the gravitational potential, which is much greater in the core of the cluster. Thus, in order to have experienced the strong tidal fields required for stream creation, singleton galaxies must be on highly radial orbits which bring them very near to the center of the cluster. Additionally, our stream detection method is biased against finding streams in galaxies which are very tightly bound to the cluster, which reside in the high-density inner regions. Due to our density-based definition of ICL, at $z = 0$ all of the luminous particles in the inner ≈ 300 kpc of the cluster are too dense to be classified as ICL, therefore any galaxy which orbits continuously within this region cannot create ICL. Galaxies

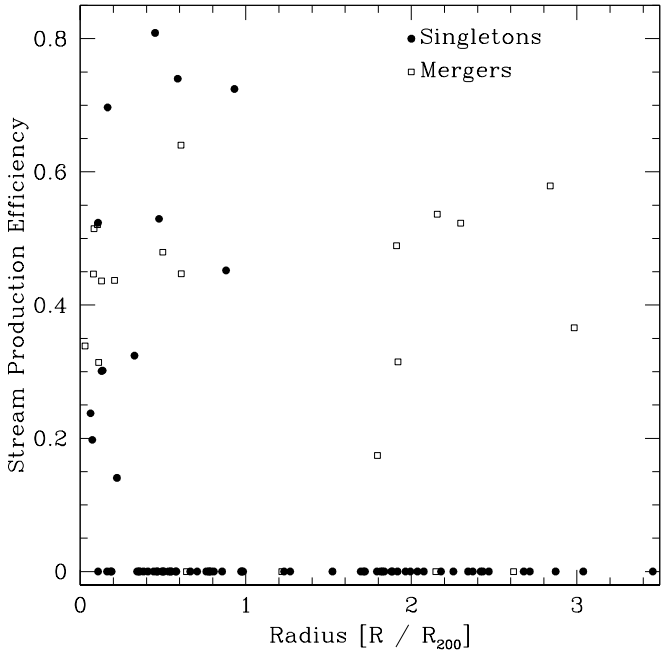

FIG. 6.— The stream production efficiency, vs. the cluster-centric radius of each galaxy at $z = 0$. Singleton galaxies (galaxies which have not undergone a merger) are represented by the solid circles and merged galaxies are represented with open squares.

that reside within this central region that have produced streams must have created those streams in an interaction that occurred before they entered the high-density cluster center. There are thus two basic scenarios for creating streams, both of which involve very close interactions between pairs of galaxies: galaxies in the process of merging; and close interactions between galaxies that do not merge, often involving the cluster cD.

The scenario outlined above is a useful, but somewhat simplistic, description of the factors which go into the production of tidal streams. The very large scatter seen in the stream production efficiencies of galaxies with similar merger, location, and orbital properties is due to the stochastic nature of the high tidal field events that create streams, and the dependence of the stripping properties on the specific dynamics of each individual case. One of the important systematic dependences affecting stream creation is the mass of the host galaxy. Our algorithm detects streams which have a minimum mass; this mass is equal to up to 9% of our least massive galaxies. Thus, low-mass galaxies require a very high fraction of their stellar mass to be stripped in a single event in order to create a stream.

5.1. *Examples of Stream Production*

In order to demonstrate some of the aspects of stream production that have been discussed above, we will show some examples of galaxies on various orbits in order to demonstrate how the specific circumstances of each galaxy affect the production of ICL streams.

5.1.1. *Galaxy Interacting with the cD*

Our first example galaxy (hereafter named galaxy G1) is a low mass disk galaxy which interacts with the cluster cD, at late times. This is a strong, fast interaction (≈ 650 km s^{-1}) with closest approach between the two

galaxies being ≈ 100 kpc. Figure 7 shows the distance between the two galaxies, and both the ICL and stream production rates of G1. The production of ICL from this event begins just after the time of closest approach, and continues to increase for some time afterward before subsiding. This is simply a generic consequence of tidal interactions between galaxies where material is compressed as the galaxies pass one another and stripped after the passage (e.g., Toomre & Toomre 1972; Hibbard & Mihos 1995). Additionally, there is no stream production until well after the ICL production has peaked, and for a short time the stream production rate is higher than the ICL production rate. This is simply due to the minimum size requirement of our stream-finding algorithm; newly created ICL particles cannot become part of a stream until there are at least 500 ICL particles which can be clustered together. Thus, a galaxy may produce ICL for a short time until a new stream is created, at which time the number of stream particles must increase by a minimum of 500, making the stream production rate artificially higher than the ICL production rate for a short time.

Figure 4 plots the luminous particles of galaxy G1 along with its stream. This galaxy displays a classic morphology seen in interactions of disk galaxies orbiting in a potential (e.g., Harding et al. 2001), with both a leading and trailing arm of tidal debris (again, only one of which we identify as a stream; see Section 3.2). We calculate the stream production efficiency of this galaxy over the time period shown in Figure 7 to be 58%, as compared with the 45% stream production efficiency of the galaxy over the entire simulation time. The fact that the stream production efficiency due to this interaction is higher than the galaxy's overall stream production efficiency indicates that this type of interaction — a fast, close encounter with a very massive galaxy — is particularly efficient at producing streams, despite the fact that a large fraction of the ICL generated is part of a cold structure, too low in mass to be a stream.

5.1.2. *Galaxy Merger Outside the Cluster*

Our second example galaxy (hereafter G2) is a massive disk galaxy which generates streams in a merger with an even more massive galaxy. This interaction occurs early in the cluster's history, at $t \approx 0.4$, before the cluster core has begun to form. The galaxy pair is relatively isolated, ≈ 2 Mpc from the other large pre-cluster groups at the time of this interaction, but will fall deep into the cluster potential by $z = 0$. The mass ratio of the merger is approximately 4:1, and the more massive galaxy is itself the product of several previous merging events.

Figure 7 shows the distance between the two galaxies, and the ICL and stream production rates of G2. As the galaxies spiral toward one another, galaxy G2 produces a large amount of ICL, almost all of which is incorporated into streams. The stream production efficiency over the time period shown is 86%. Due to the fact that this galaxy merges with another, and therefore no longer exists as an independent entity after the merger, we cannot calculate the stream production efficiency of the galaxy over the entire simulation time. However, the fact that this event's stream production efficiency is higher than that seen for any galaxy over the course of the entire simulation (see Figure 6) suggests that this type of merging event is particularly efficient at generating streams.

Figure 4 shows the streams produced by this galaxy, two of which are very massive (shown in red and blue, respectively) while the other is of lower mass (shown in green). A more detailed analysis of the history of these streams reveals that the two massive streams were generated by two subsequent close encounters of the galaxy pair as they spiraled together. All of these streams show a generally long, thin morphology similar to that seen in the streams from galaxy G1.

5.1.3. *Galaxy Merging with the cD*

Our final example galaxy (hereafter G3) is a very massive elliptical, the product of numerous mergers, that is merging with the even more massive cluster cD. Figure 7 shows the distance between G3 and the cD, as well as the ICL and stream production rates of G3. The stream production efficiency over the time period shown is only 30%, meaning that this type of interaction is much less efficient at producing streams than the two examples previously discussed. This galaxy exists in an extremely complex, dynamically hot environment, which is not conducive to the creation of dynamically cold structures. Additionally, as this galaxy is a massive elliptical galaxy produced by the merger of numerous galaxies, its stellar material, even before it is stripped from the galaxy to form ICL, is likely to be much more dynamically hot than the cold disks which we examined in the previous examples.

Figure 4 shows galaxy G3 and its streams. Both of the streams exist on the left side of the galaxy, as it has just had a close encounter with the cD, moving from right to left. This is an example of the fact that using our ICL definition, ICL, and therefore streams, cannot be created in the high-density center of the cluster. Thus the streams are on the low-density side of the galaxy, away from the cD. The morphology of these streams, which look like plumes or shells, is qualitatively very different from the long thin structures seen in the previous two examples which were much farther from the cluster center. The following section will examine more quantitatively how streams found in diverse environments evolve differently.

6. THE LIFE OF STREAMS

In the previous section we saw that tidal streams that form in varying circumstances tend to have different morphologies. We would expect that these diverse environments should also affect the evolution of the streams themselves. In this section we will examine more quantitatively how streams found in diverse environments evolve differently, and measure the time it takes for streams to dissolve into the diffuse ICL background.

In order to follow the growth and decay of an individual stream, we first have to be able to identify and track the stream as it evolves through time. The situation is similar to, but somewhat more complex than, the case of following dark matter halo assembly histories in a hierarchical universe (e.g., Wechsler et al. 2002), with streams continually gaining and losing particles, and sometimes merging together or splitting into multiple pieces. Unfortunately, the complexity of the processes makes it prohibitively difficult for us to simply search through the primary stream catalog and determine each stream's progenitor(s) and offspring. We therefore employ an alter-

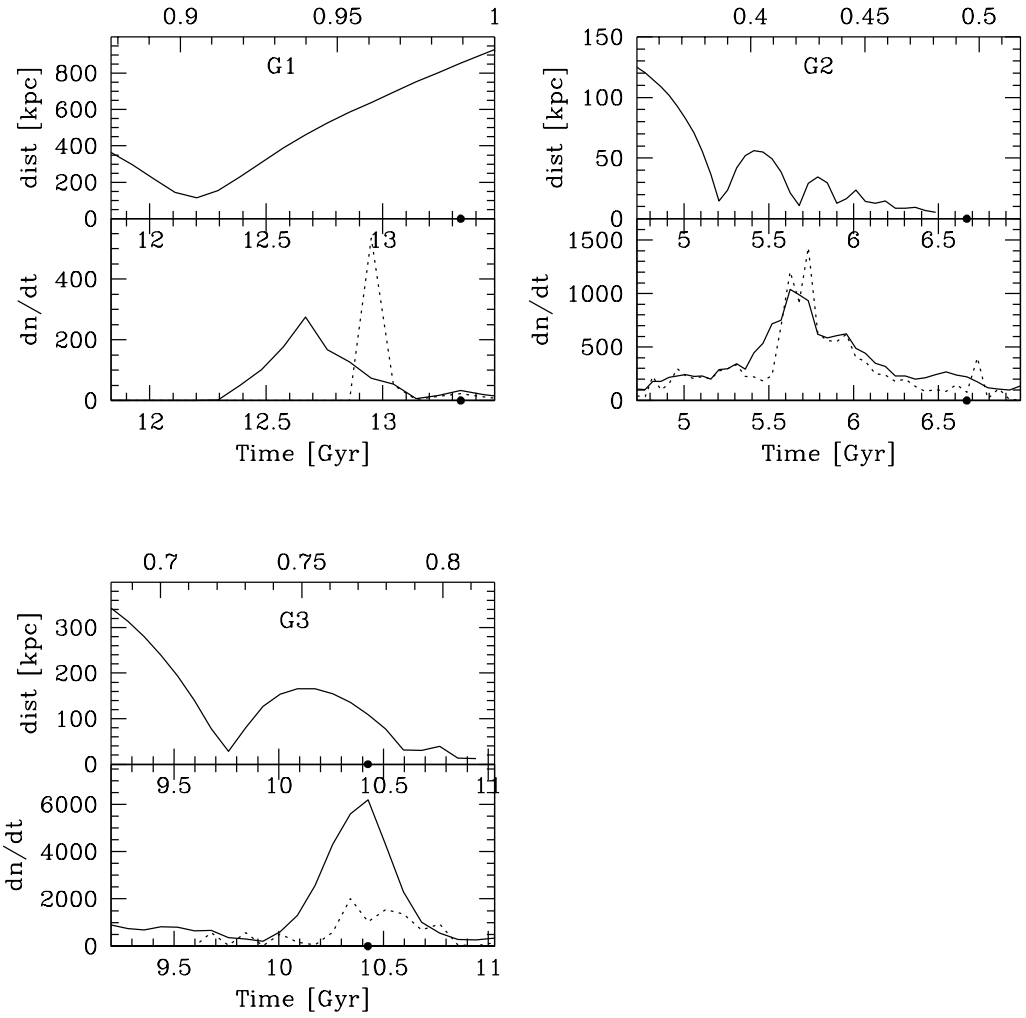

FIG. 7.— The three subfigures represent the three galaxies G1, G2, and G3, respectively. Top: the distance between the galaxy in question and the galaxy with which it is merging (G2 and G3) or the cD (G1). Bottom: the ICL (solid line) and stream (dotted line) production rates, for each individual galaxy, in units of particles per timestep. The bottom time axes show the age of the universe in physical time units. However, the top time axis of each plot is fraction of the age of the universe, as in Figure 5. The dots along the time axes mark the time when the galaxy is shown in Figure 4.

native method, where we follow the evolution of each stream by eye, in order to determine when the stream reaches its maximum size. In the majority of cases, the evolution of the stream is easy to determine, as it simply gains or loses a small fraction of its particles each timestep. In situations where multiple streams merge together, or a single streams splits into multiple pieces, we have to make a somewhat subjective choice as to the true identity of the stream. However, our subsequent analyses are not greatly affected by these choices, as at this stage we are simply identifying the timepoint, t_{max} at which the stream reaches its maximum size. Once we have identified t_{max}, we select the particles which comprise the stream at this time and then re-run the clustering algorithm at all timesteps using only this subset of particles. Thus, we can follow the evolution of the stream by tracking a well-defined particle subset.

Figure 8 shows the evolution of a few typical streams from the simulation. We have measured the size of the streams in two different ways: the largest group of clustered particles, and the aggregate size of all clustered groups of particles. The measurement method used does not have a strong effect on our basic conclusions, and all analyses shown measure cluster size using the largest remaining cluster.

In almost all cases, the streams grow very quickly to their maximum size and then slowly decay as the stream dissolves into the global ICL background, or simply disperses until it is to low in density to be identified by our algorithm. Unsurprisingly, the rapid initial growth of the streams indicates that the vast majority of the stream particles become ICL as a result of a single tidal stripping event that creates the stream (particles can only be clustered together into a stream once the particles have become ICL).

More interesting is the decay of the streams as they gradually lose particles. There is wide variation in the timescale over which streams decay, with some decaying quickly and others more slowly. In order to quantitatively measure the timescales on which these streams decay, we have modeled the decay as an exponential decay process, of the form:

$$n \propto e^{-t/\tau} \tag{2}$$

where n is the size of the stream, t is the time, and τ is the characteristic decay time of the stream. The value

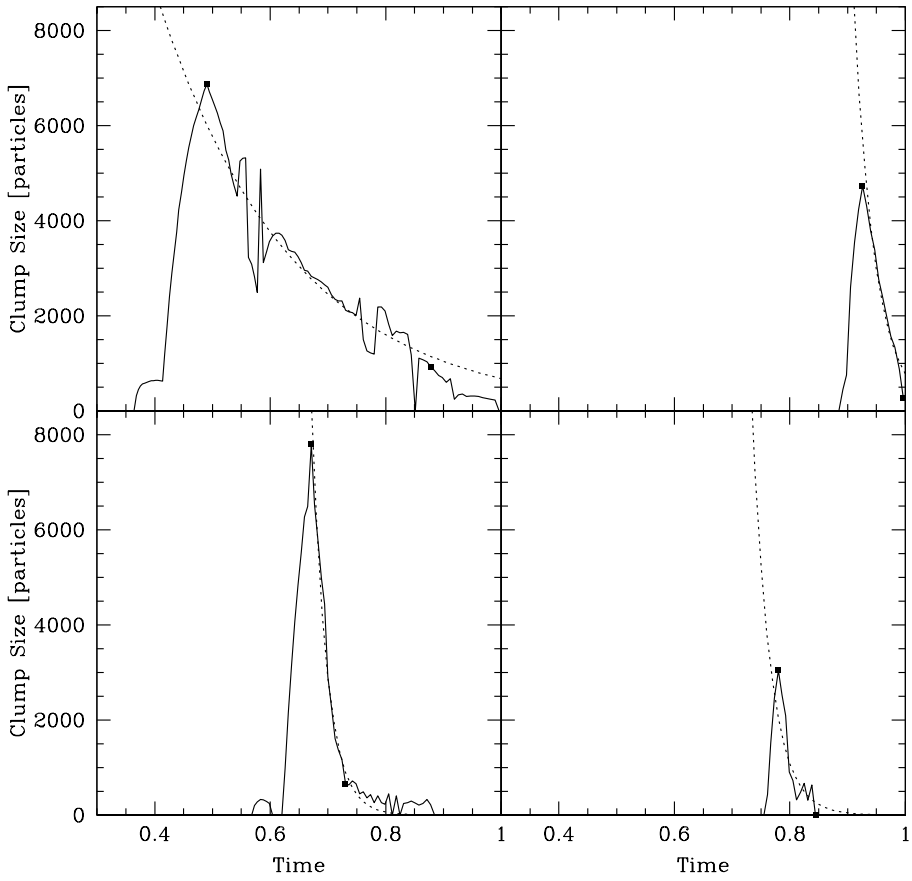

FIG. 8.— SOLID LINES: The size of four example streams as a function of time. DOTTED LINES: The fitted exponential decay of each stream. SQUARES: The times between which the decay curves were fit, t_{max} and the time when the stream size had decreased by at least 2 e-foldings from the maximum (see text for details).

of τ is obtained by a least squares fit to the data, using the data from time t_{max} until the time when the stream size had decreased by at least two e-foldings from the maximum, and stayed below this size for at least two consecutive timepoints. Streams which form at late times which do not decay by at least one e-folding by $z = 0$ are excluded; streams which decayed by between one and two e-foldings are fitted between time t_{max} and $z = 0$. This analysis was restricted to only the largest streams, which reached a size of at least 2000 particles, corresponding to a stellar mass of 2.8×10^9 $M_\odot$, to ensure that we could robustly measure their decay. In addition, we relax our constraint of having at least 500 particles in a stream for the descendants of these large streams to ensure we fit over at least two e-foldings in mass decay. The fits for our example streams are shown in Figure 8. A small number of streams have decay times that are not possible to accurately fit, and are excluded from all further analyses. These streams generally have complex evolutionary histories due to the fact that they are created not from a single stripping event, but from multiple events occurring in rapid succession, and should therefore be thought of as multiple independent streams, but are nonetheless aggregated into a single stream by our clustering algorithm.

Figure 9 shows the decay time, τ, for each stream versus the dynamical time of the stream in the cluster, given by

$$t_{dyn} = \frac{\pi}{2}\sqrt{\frac{r^3}{GM}} \quad (3)$$

where r is the stream's cluster-centric radius and M is the mass enclosed within this radius (Binney & Tremaine 1987). The dynamical time is driven primarily by the stream's cluster-centric radius, determined to be the distance from the cluster center of mass to the mean position of the stream particles at time t_{max}. There are two major sources of uncertainty in the calculation of t_{dyn}: the cluster center of mass is not well defined, especially at early times; and the streams are often both highly extended and have high velocities, making their cluster-centric radius somewhat ambiguous. Despite the large uncertainties that accompany both the measurement of the decay time and the dynamical time, there clearly is a correlation between the two, with the decay time being approximately 1.5 times the dynamical time. Essentially, we find that streams which are found in the core of the cluster, with short dynamical times, are quickly destroyed by the strong, evolving tidal field of the cluster, with $\tau \lesssim 1$ Gyr. Streams found farther outside of the cluster are not subject to these tidal fields, and decay more slowly, with decay times up to several gigyears in length. There is a small cluster of points at $t_{dyn} \approx 0.3$ and $\tau \approx 1.2$ which lie somewhat above this relationship. Each of these streams is formed at $t \approx 0.6 - 0.7$ in the extremely complex environment of the collapsing cluster core. At this time, the cluster potential is rapidly chang-

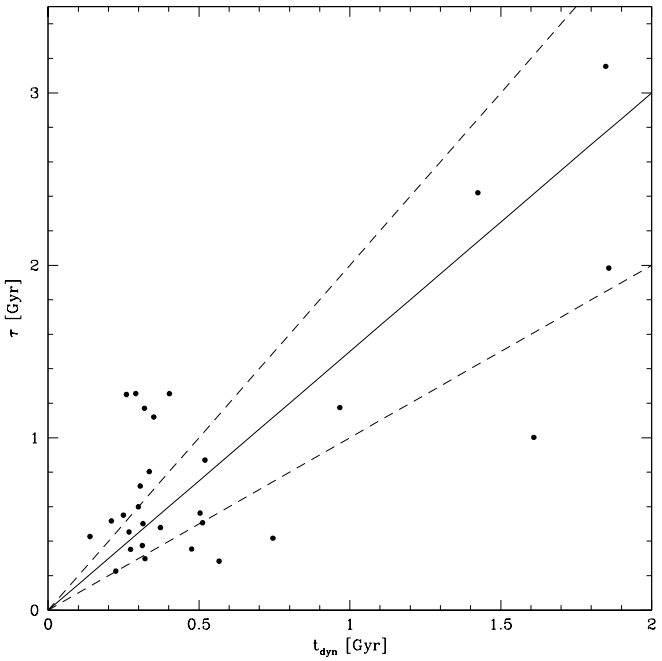

FIG. 9.— The decay time, τ, vs. the dynamical time, t_{dyn} for each stream. The solid line shows relation $\tau = 1.5t_{dyn}$, while the dashed lines follow $\tau = t_{dyn}$ and $\tau = 2t_{dyn}$, respectively.

ing which can significantly bias our determination of the dynamical timescale.

These data indicate that the evolution of streams is primarily determined by the external cluster environment where they are found. In the cluster core, where dynamical times are short and tidal fields are strong, streams decay rapidly, whereas outside the cluster they decay more slowly. However, there are numerous other variables, such as the velocity and orbit of the stream, the stream morphology, etc., which will contribute to stream's evolution.

7. SUMMARY AND DISCUSSION

In this paper we have identified tidal streams of ICL, calculated their contribution to the cluster's total ICL, studied the galactic interactions which give rise to them, and measured their decay properties. We have used a density-based definition of ICL, based on a density threshold below which particles are classified as ICL, in order to quantify the ICL component using a simple, repeatable measurement. Our stream identification algorithm is a friends-of-friends-type clustering algorithm, which is able to detect streams using six-dimensional phase space information to find groups of particles from a common parent galaxy which share similar positions and velocities.

We find that early in the cluster's history, the majority of ICL is produced in massive, dynamically cold tidal streams, while at later times a smaller fraction of ICL is produced in streams. However, as in R06, we find that the production of ICL is episodic, suggesting that it is dominated by discreet events, irrespective of these events efficiency at forming streams. Overall, we calculate that $\approx 40\%$ of the cluster's ICL is generated in streams. We find that merging pairs of galaxies are relatively efficient at producing streams because of the strong tidal fields that are created during the merging process. However, galaxies which do not undergo a merger are much less likely to produce streams, and in order to do so must have a very close encounter with a massive galaxy, often the cluster cD. Once a stream is created, it begins to lose mass and decay due to the cluster tidal field. We calculate the decay time of streams to be ≈ 1.5 times the dynamical time of the stream in the cluster.

The stream-finding algorithm we have employed in this paper is sensitive only to relatively high-density, high-mass ($M \geq 7.0 \times 10^8$ M$_\odot$) streams. ICL substructures which are too low in mass or density to be identified as streams by our algorithm, such as the examples seen in Figure 4, are likely to contain similarly useful information as the streams we have identified. However, these low mass or density structures are also likely to be more difficult to detect observationally. Similarly, due to our initialization scheme, we are not able to identify ICL substructures created by galaxies below our minimum galaxy mass limit (6×10^{10} M$_\odot$). Although these low mass galaxies contribute only a small amount of the cluster's luminosity, their large numbers have the potential to make their ICL substructure particularly useful in studying the cluster's history and dynamics.

Together, these data suggest a scenario where the dominant mechanism driving the formation of ICL is highly dependent on the dynamical state of the cluster. Early in the cluster's history, when galaxies are mostly found in small groups which have yet to merge into a single cluster potential, stream production dominates. The interactions that are occurring tend to be close encounters within the group environment, often involving merging events which are efficient at generating tidal streams, as with galaxy G2. Additionally the relatively weak group potentials found in these environments are ineffective at dissolving streams, as evidenced by the correlation between a stream's decay time and its dynamical time in the cluster. However, as time passes and the cluster potential grows, we see a different behavior where ICL is less likely to be generated in large tidal streams. As we saw with galaxy G3, the mergers of massive galaxies deep in the cluster potential are much less effective at generating tidal streams, due to the complex tidal field of the cluster potential as well as the fact that the stellar material of these galaxies has already been significantly heated during their formation. The streams that result are rapidly dissolved by the cluster potential.

This scenario is consistent with the findings of R06, which found that at early times, the morphology of the ICL is dominated by long, linear features, whereas at late times the ICL became a more diffuse, amorphous envelope within the cluster. The long, linear features are the tidal streams which are created in the group environment early in the cluster's evolution. The diffuse envelope seen at late times is created from tidal stream which have been dissolved by the cluster, as well as the high fraction of ICL which at late times is not produced in streams.

We can use this scenario to potentially interpret observational data of cluster ICL. In a highly evolved, dynamically old cluster, we would expect the ICL to show a morphology dominated by a diffuse envelope, with relatively few streams. Those streams that do exist will be relatively short lived, indicating that they were created by events in the very recent history of the cluster. In con-

trast, a dynamically young cluster dominated by galaxy groups still in the process of merging is likely to have a higher fraction of its ICL found in streams.

The structure of ICL streams found in a galaxy cluster can help us to understand not only the properties and evolution of the cluster itself, but also give us information on the galaxies in the cluster. We have seen that dynamically hot elliptical galaxies tend to produce streams with morphologies such as shells or plumes which are qualitatively different than the long thin tail-like streams produced by cold disk galaxies. Therefore, the observed morphology of a stream is related to the type of galaxy which created it. Additionally, because streams are created by specific events, such as close galactic encounters, a galaxy's streams can tell us about its orbital history. For example, while galaxy G1 is ≈ 800 kpc from the cD at the time it is seen in Figure 4, its streams give an indication that it has recently had a major interaction with one of the cluster's massive galaxies.

Thus, we find that not just the quantity, but the structure, of the ICL is a useful tool in understanding the evolution and dynamics of galaxy clusters. Many of the relevant substructures we have discussed have very low surface brightnesses and may only be detectable by incorporating kinematic measurements of the ICL, such as ongoing planetary nebulae studies. Such analyses have the potential to greatly increase our knowledge of the processes that drive galaxy cluster evolution.

C.S.R. appreciates support from the Jason J. Nassau Graduate Fellowship Fund. J.C.M. acknowledges research support from the NSF through grants ASTR 06-07526 and ASTR 07-07793. This work utilized the computing resources of the CWRU ITS High Performance Cluster.

REFERENCES

Aguerri, J. A. L., Gerhard, O. E., Arnaboldi, M., Napolitano, N. R., Castro-Rodriguez, N., & Freeman, K. C. 2005, AJ, 129, 2585
Aguerri, J. A. L., Castro-Rodríguez, N., Napolitano, N., Arnaboldi, M., & Gerhard, O. 2006, A&A, 457, 771
Arnaboldi, M., Gerhard, O., Aguerri, J. A. L., Freeman, K. C., Napolitano, N. R., Okamura, S., & Yasuda, N. 2004, ApJ, 614, L33
Belokurov, V., et al. 2006, ApJ, 642, L137
Berlind, A. A., & Weinberg, D. H. 2002, ApJ, 575, 587
Binney, J., & Tremaine, S. 1987, Galactic Dynamics, Princeton, NJ, Princeton University Press, 1987, 747 p.,
Byrd, G., & Valtonen, M. 1990, ApJ, 350, 89
Calcáneo-Roldán, C., Moore, B., Bland-Hawthorn, J., Malin, D., & Sadler, E. M. 2000, MNRAS, 314, 324
Conroy, C., Wechsler, R. H., & Kravtsov, A. V. 2007, ApJ, 668, 826
Da Rocha, C., & Mendes de Oliveira, C. 2005, MNRAS, 364, 1069
Da Rocha, C., Ziegler, B. L., & Mendes de Oliveira, C. 2008, MNRAS, 388, 1433
Durrell, P. R., Ciardullo, R., Feldmeier, J. J., Jacoby, G. H., & Sigurdsson, S. 2002, ApJ, 570, 119
Ester, M., Kriegel, H., Sander, J., Xu, X. 1996, in Proc. 2nd Int. Conf. of Knowledge Discovery and Data Mining (KDD-96), ed. Evangelos Simoudis, Jiawei Han, and Usama Fayyad (Menlo Park, CA: The AAAI Press)
Feldmeier, J. J., Ciardullo, R., & Jacoby, G. H. 1998, ApJ, 503, 109
Feldmeier, J. J., Mihos, J. C., Morrison, H. L., Harding, P., Kaib, N., & Dubinski, J. 2004, ApJ, 609, 617
Feldmeier, J. J., Mihos, J. C., Morrison, H. L., Rodney, S. A., & Harding, P. 2002, ApJ, 575, 779
Ferguson, H. C., Tanvir, N. R., & von Hippel, T. 1998, Nature, 391, 461
Gal-Yam, A., Maoz, D., Guhathakurta, P., & Filippenko, A. V. 2003, AJ, 125, 1087
Gerhard, O., Arnaboldi, M., Freeman, K. C., Kashikawa, N., Okamura, S., & Yasuda, N. 2005, ApJ, 621, L93
Gnedin, O. Y. 2003, ApJ, 582, 141
Gonzalez, A. H., Zabludoff, A. I., & Zaritsky, D. 2005, ApJ, 618, 195
Gregg, M. D., & West, M. J. 1998, Nature, 396, 549
Harding, P., Morrison, H. L., Olszewski, E. W., Arabadjis, J., Mateo, M., Dohm-Palmer, R. C., Freeman, K. C., & Norris, J. E. 2001, AJ, 122, 1397
Hernquist, L. 1993, ApJS, 86, 389
Hernquist, L. 1990, ApJ, 356, 359
Hibbard, J. E., & Mihos, J. C. 1995, AJ, 110, 140
Johnston, K. V., Bullock, J. S., Sharma, S., Font, A., Robertson, B. E., & Leitner, S. N. 2008, ApJ, 689, 936
Jurić, M., et al. 2008, ApJ, 673, 864
Krick, J. E., Bernstein, R. A., & Pimbblet, K. A. 2006, AJ, 131, 168
Krick, J. E., & Bernstein, R. A. 2007, AJ, 134, 466
Merritt, D. 1984, ApJ, 276, 26
Mihos, J. C. 2004, in Clusters of Galaxies: Probes of Cosmological Structure and Galaxy Evolution,ed. J. S. Mulchaey, A. Dressler, and A. Oemler (Cambridge: Cambridge Univ. Press), 277
Mihos, J. C., Harding, P., Feldmeier, J., & Morrison, H. 2005, ApJ, 631, L41
Monaco, P., Murante, G., Borgani, S., & Fontanot, F. 2006, ApJ, 652, L89
Moore, B., Katz, N., Lake, G., Dressler, A., & Oemler, A. 1996, Nature, 379, 613
Murante, G., et al. 2004, ApJ, 607, L83
Murante, G., Giovalli, M., Gerhard, O., Arnaboldi, M., Borgani, S., & Dolag, K. 2007, MNRAS, 377, 2
Napolitano, N. R., et al. 2003, ApJ, 594, 172
Neill, J. D., Shara, M. M., & Oegerle, W. R. 2005, ApJ, 618, 692
Nishiura, S., Murayama, T., Shimada, M., Sato, Y., Nagao, T., Molikawa, K., Taniguchi, Y., & Sanders, D. B. 2000, AJ, 120, 2355
Purcell, C. W., Bullock, J. S., & Zentner, A. R. 2007, ApJ, 666, 20
Rudick, C. S., Mihos, J. C., & McBride, C. 2006, ApJ, 648, 936 (R06)
Saro, A., Borgani, S., Tornatore, L., De Lucia, G., Dolag, K., & Murante, G. 2009, MNRAS, 392, 795
Sommer-Larsen, J. 2006, MNRAS, 369, 958
Sommer-Larsen, J., Romeo, A. D., & Portinari, L. 2005, MNRAS, 357, 478
Springel, V., Yoshida, N., & White, S. D. M. 2001, New Astronomy, 6, 79
Stanghellini, L., González-García, A. C., & Manchado, A. 2006, ApJ, 644, 843
Toomre, A., & Toomre, J. 1972, ApJ, 178, 623
Trentham, N., & Mobasher, B. 1998, MNRAS, 293, 53
Uson, J. M., Boughn, S. P., & Kuhn, J. R. 1991, ApJ, 369, 46
Vilchez-Gomez, R., Pello, R., & Sanahuja, B. 1994, A&A, 283, 37
Wechsler, R. H., Bullock, J. S., Primack, J. R., Kravtsov, A. V., & Dekel, A. 2002, ApJ, 568, 52
White, P. M., Bothun, G., Guerrero, M. A., West, M. J., & Barkhouse, W. A. 2003, ApJ, 585, 739
Williams, B. F., et al. 2007b, ApJ, 654, 835
Williams, B. F., et al. 2007a, ApJ, 656, 756
Willman, B., Governato, F., Wadsley, J., & Quinn, T. 2004, MNRAS, 355, 159
Zibetti, S., White, S. D. M., Schneider, D. P., & Brinkmann, J. 2005, MNRAS, 358, 949
Zwicky, F. 1951, PASP, 63, 61